RELATIONSHIP BETWEEN ELECTRICAL CONDUCTIVITY AND SPATIAL STRUCTURE OF CAPILLARY PORES IN CEMENT PASTES

Shin-ichi Igarashi*

Kanazawa University, Kanazawa, JAPAN.

*: corresponding author. igarashi@se.kanazawa-u.ac.jp

ABSTRACT

Electrical conductivities of hardened cement pastes were investigated in relation to spatial structure of coarse capillary pores. There exists a good correlation between the porosity and the electrical conductivity in ordinary cement pastes. Spatial statistics for the coarse pores were also positively correlated to the porosity. Connectivity of invisible fine capillary pores seemed increasing events with the fine porosity. On the other hand, the conductivity was less correlated to the spatial structure of coarse pores in cement pastes with mineral admixtures. The conductivity was smaller for the coarse porosity in the cement pastes. Connectivity that used fine pores as effective paths was decreased by the incorporation of mineral admixture.

Keywords: capillary pores, spatial statistics, electrical conductivity, connectedness

INTRODUCTION

Because of its porous nature, properties of concrete are greatly influenced by its pore structure, regardless of ages and materials used for the concrete. Many analytical techniques have been used to investigate microstructure such as pore structure in concrete. SEM-BSE image analysis is a sophisticated technique, which has been successful in evaluating the hydration process of cement or microstructural gradients in concrete quantitatively. However, there have been few studies to apply this technique directly to elucidating durability problems in concrete [1].

In general, the volume, sizes and continuity of pores above a certain size are to be the relevant quantities for determining various properties of concrete. Therefore,

characteristics of capillary pore structure revealed by the imaging method must be closely related to not only mechanical but also durability issues such as permeability. However, for example, presence of pores larger than the critical diameter is ignored when permeability or conductivity is discussed based on MIP curves and percolation theory [2]. Pores detected in SEM-BSE technique fall exactly into a range of those discarded pores. It is generally believed that permeability is dominantly controlled by fine capillary pores or their connectivity as bottlenecks. However, pore structure or its network in cement paste practically consists of variety sizes of pores, which connect each other. The observed large pores can be cross sections of effective paths consisting of interconnected pores. Indeed, Wong et al [1] have shown that transport properties of mortars can be correlated to the quantitative information on those large pores detected by the SEM-BSE image analysis. They have concluded that the large pores in the image analysis can be used as input data for the transport model in concrete. This approach is quite contrary to a traditional interpretation of the MIP examination.

In this study, electrical conductivity testing was used to evaluate a transport property of cement pastes. Relationship between the electrical conductivity and characteristics of capillary pore structure revealed by the SEM-BSE image analysis was investigated with an emphasis on pore connectivity. Effects of water/binder ratios and mineral admixtures on the conductivity were discussed in terms of spatial correlation and statistics for the entire pore structure.

EXPERIMENTS

(1) Materials and mix proportion of cement pastes

The cement used was ordinary Portland cement (OPC) with a Blaine fineness of 3310cm^2/g. A commercial silica fume (SF) with a specific surface area of 20m^2/g and a local fly ash (FA) with the fineness of 3450cm^2/g were used as mineral admixtures. Water/binder ratios of cement pastes were 0.25, 0.40, 0.50 and 0.60. The replacement levels of silica fume and fly ash were 10% and 15%, respectively. A polycarboxylic acid type superplasticizer was used in cement pastes with the water/binder ratio of 0.25. Cylindrical specimens of two sizes of 100 and 200mm in length and 50 and 100mm in diameter were produced in accordance with JIS R 5201 and JSCE-F506. They were demolded at 24 h after casting, and then cured in water at 20˚C.

(2) BSE image analysis

At the prescribed ages, slices about 10 mm thick were cut from the small cylinder specimens for the BSE image analysis. They were dried by ethanol replacement and vacuum freeze-drying with t-butyl alcohol, and then impregnated with a low viscosity epoxy resin. After the resin hardened at room temperature, the slices were finely polished. The polished surfaces were finished with a diamond slurry.

Samples were examined using an SEM equipped with a quadruple backscatter detector. BSE images were acquired at a magnification factor of 500×. Each BSE image consists of 1148×1000 pixels. The size of one pixel is about 0.22 μm×0.22 μm. Capillary pores range widely in size from nm to mm. The pixel size falls in a range of larger capillary pores. Thus, the pores tallied in the image analysis are termed coarse capillary pores. Pixels for residual unhydrated cement particles and the coarse pores were counted in order to obtain the area fractions of these two phases. The degree of hydration of cement was calculated by comparing the area fraction of unhydrated cement with the initial volume of cement.

(3) Electrical conductivity

At the prescribed ages, discs of 100mm in diameter and 50mm in thickness were cut from the larger specimens. After the saturation treatment was done in accordance with JSCE G571, electrical conductivity (σ) of the disc specimens was measured using equipment of ASTM C 1202. As proposed by Nokken and Hooton [3], applied voltage was 30V, and sodium hydroxide solution of 0.3N was put in the cell chambers. Bulk conductivity was calculated using Eq.(1);

$$\sigma = \frac{I \cdot L}{V \cdot A} \tag{1}$$

Where I is the current, L is the thickness of the disc specimen, V is the voltage applied to the equipment, and A is the cross-sectional area of the specimen. The measured conductivity (σ) was normalized by the conductivity (σ_0) of pore solution for each specimen. It was calculated using the Taylor model [4] and the Snyder et al model [5].

(4) Loss on ignition and insoluble residue

Small portions of hardened cement pastes were taken from the small cylinder specimens. Loss on ignition and an insoluble residue were obtained in accordance with JIS R 5202.

(5) Degree of reaction of fly ash and silica fume

The amounts of unreacted fly ash and silica fume were calculated using the results of insoluble residue. The insoluble residue was corrected using losses on ignition for the admixtures and the cement themselves [6]. Comparing the initial amounts of the admixtures with the residues, degrees of pozzolanic reaction were calculated [6].

(6) Calculation of capillary porosity

Capillary porosities of cement pastes were calculated using the degree of hydration and the Powers-Brownyard model. For the pozzolanic reaction, the following equation was assumed [7];

$$S + 1.5CH + 2.3H \rightarrow C_{1.5}SH_{3.8} \tag{2}$$

It was also assumed that C-S-H produced by the pozzolanic reaction had the same property as the one produced by the hydration of cement. The amount of C-S-H produced by the pozzolanic reaction was calculated using Eq.(2) and the degree of pozzolanic reaction. The entire porosity was obtained by subtracting those solid products and unreacted binders from the whole volume of cement paste. Difference between the entire porosity and the coarse capillary porosity evaluated by the image analysis was regarded as porosity smaller than the image resolution. This is termed fine capillary porosity.

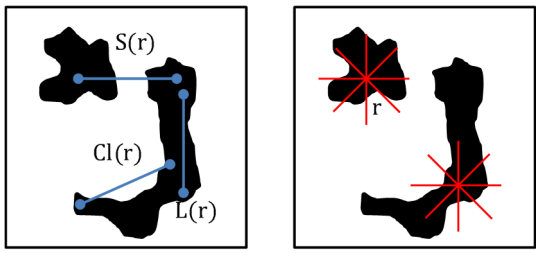

(a) (b)

(7) Calculation of spatial statistics

The two-point correlation function (covariance function) S(r) and the lineal-path function L(r) for the coarse capillary pore phase are obtained from the binary images of extracted pores (Fig.1(a)) [8]. The former is a probability function that both endpoints of a line segment of length r hit the pore phase. The latter was a function that the line segment of length r was fully within the pore phase. With regard to S(r), the cluster correlation function Cl(r) was also calculated. This is a specific case of S(r) such that the two endpoints of a line segment belong to the same cluster of the pore phase (Fig. 1(a)). To calculate these functions, templates with eight radial directions were repeatedly placed on the images (Fig. 1(b)). From these functions, parameters of length scales, λ, ζ and ξ were calculated.

$$\lambda = \int_0^\infty [S(r) - \{S(0)\}^2]dr \qquad (3)$$

$$\zeta = \int_0^\infty rL(r)dr \qquad (4)$$

$$\xi^2 = \frac{\int_0^\infty r^2 Cl(r)dr}{\int_0^\infty Cl(r)dr} \qquad (5)$$

A parameter λ represents the probability of positive correlation. It is related to fluid permeability of a porous media. A parameter ζ is the first moment of L(r), which expresses the average length of lineal continuity in the pore phase. A parameter ξ is called correlation distance in the percolation theory.

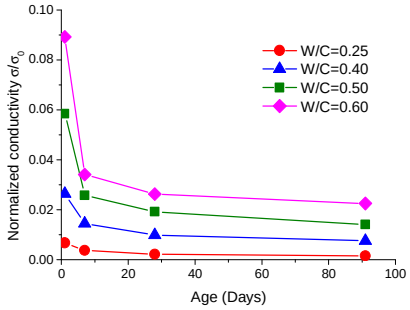

Fig.2 Normalized conductivity of ordinary cement pastes

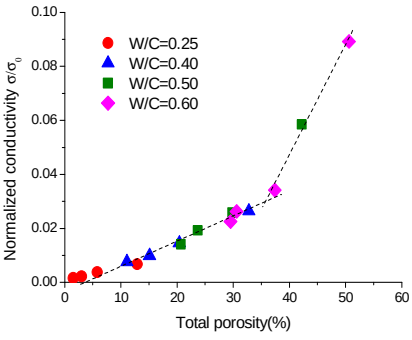

Fig.3 Conductivity vs. total porosity in ordinary cement pastes

RESULTS AND DISCUSSION

(1) Changes in electrical conductivity with time

Fig.2 shows normalized conductivities of ordinary cement pastes. They decreased with time, as expected. The larger the water/cement ratio, the greater reduction in conductivity at early ages.

Figs. 3 and 4 show relationships between normalized conductivity and the entire capillary porosity, and coarse capillary porosity, respectively. The normalized conductivity was approximated by two regression lines. This suggests that once the porosity is beyond a certain value, the conductivity increases discontinuously. Furthermore, a resemblance between the two figures also suggests the coarse pore structure may have a similarity to the entire pore system. This means the coarse pore structure can be a sample to estimate a transport property of cement pastes. It should be noted that characteristic porosities at which a rate of increase in the conductivity changes discontinuously are about 0.20 for the coarse porosity and 0.35 for the entire porosity, respectively. The former is closer to the theoretical value of percolation threshold in porosity for cement paste [9]. This suggests that most of the coarse porosity may be effectively connected to a backbone of conductivity paths. In other words, the coarse porosity contains less dead-end or isolated pores, which do not contribute to the conductivity.

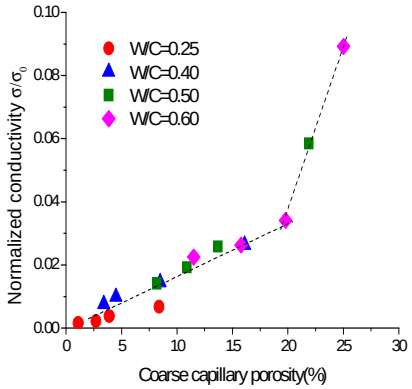

Fig.4 Conductivity vs. coarse porosity in ordinary cement pastes

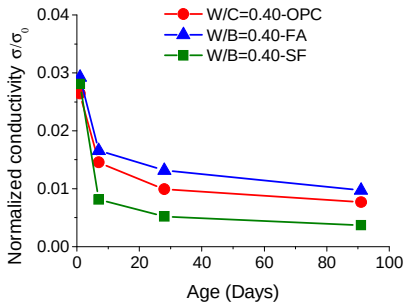

Fig.5 Comparison of normalized conductivity between cement pastes with and without admixtures

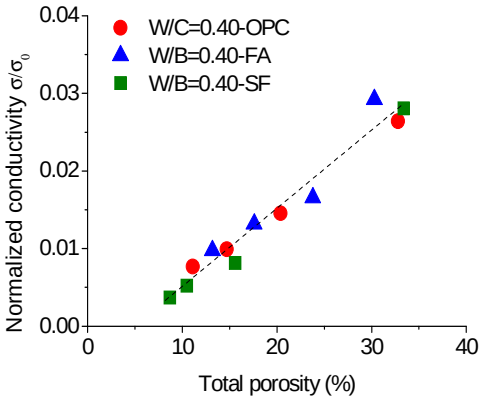

Fig.6 Conductivity vs. total porosity in cement pastes with mineral admixtures

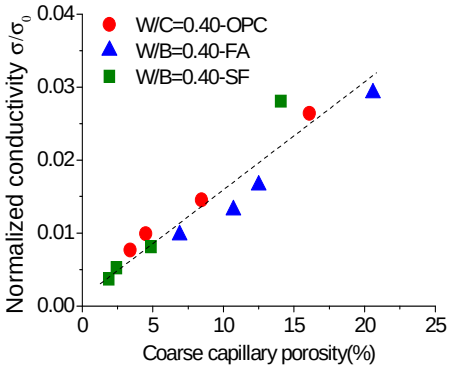

Fig.7 Conductivity vs. coarse porosity in cement pastes with mineral admixtures

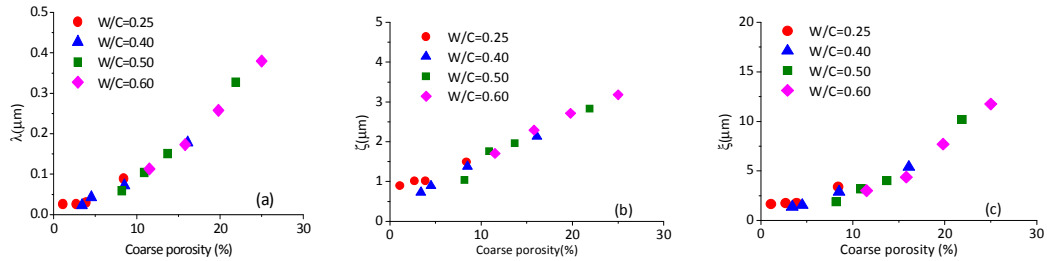

Fig.8 Characteristic parameters vs. coarse capillary porosity in ordinary cement pastes

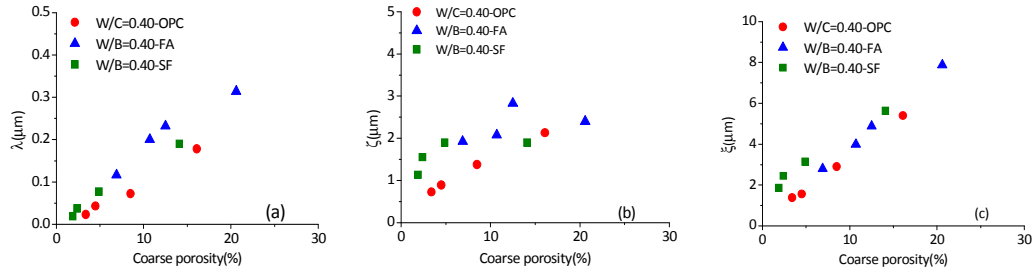

Fig.9 Characteristic parameters vs. coarse capillary porosity in cement pastes with mineral

Fig.5 shows the normalized conductivity of cement pastes with the mineral admixtures. The addition of silica fume reduces the conductivity. However, the conductivity of pastes with fly ash is always greater than that of the plain cement pastes. Figs.6 and 7 show relationships between the conductivity and the porosities in the cement pastes with the admixtures. There exists a good correlation between them as well as in the plain cement paste (Figs. 3 and 4).

(2) Reflection of path continuity to coarse capillary pore structure

As shown in Figs. 4 and 7, there exist a good correlation between the conductivity and the coarse capillary porosity. Then, a simple equation such as Eq.(6) can be valid for those cement pastes [10].

$$\sigma = \sigma_0 \beta \phi \tag{6}$$

Where β is a coefficient representing geometrical features of pores, ϕ is a porosity. The porosity in Eq.(6) should be the one which actually contributes to conductivity as effective paths. Taking account of the fact that Eq.(6) can be applied to a coarse capillary porosity which is just a subset of the entire porosity, the following two things are suggested. The first is that fine pores are less effective to the entire conductivity. In other words, the probability of disconnection or closure is higher in those fine capillary pores. For example, the entire porosity calculated by the Powers and Brownyard model is about twice as large as the coarse porosity, as found from Figs.3 and 4. Nevertheless, the subset of the entire pores can represent the conductivity of the entire system. Therefore, fine pores are less relevant to the conductivity whereas the coarse porosity plays a vital role as the interconnected path for the conductivity. The second is there exists similarity in continuity or spatial correlation between the coarse and fine pore structures. The conductivity depends on not only the amount of pores but also their connectivity or spatial continuity. Fig. 8 shows relationships between pore parameters and the coarse porosity. Positive correlations to the porosity were

observed for all the parameters. The greater the porosity, the greater continuity and connectivity of pores through lineal or tortuous paths the pore structures have. Furthermore, in view of positive correlation between the entire porosity and the conductivity, fine pore structure does not dominate the entire continuity. In other words, any fine pore structure does not upset the conductivity which is formed by geometrical features of coarse pore structures. The greater the fine porosity, the more continuity or connectivity the fine pore structure has. As a result, the coarse pore structure is representative of the entire pore system with regard to transport properties.

(3)Effects of mineral admixtures on spatial structure of pores

In general, pore systems with mineral admixtures are expected to have more disconnected networks of pores. In this study, however, fly ash did not decreased the conductivity less than the plain pastes while silica fume decreased it. Relationships between the entire or coarse porosities and the conductivity were plotted on the same regression line as the plain paste (Figs.6 and 7). Fig.9 shows the spatial parameters for coarse pores in cement pastes with the admixtures. Compared to the plain pastes (Fig.8), correlations of each parameter with the coarse capillary porosity are not clearly seen. The parameter λ of the systems with the admixtures is always greater than the plain. The parameter ζ did not appreciably change with time so that they were greater than the plain as a whole. The parameter ξ for the silica fume system was also greater than the plain in the range of smaller diameters. In summary, as long as the coarse pore structures are observed, spatial correlation for coarse pores in the admixture-containing pastes is greater than in the plain. Therefore, conductivity of cement pastes with the admixtures is expected to increase beyond the plain pastes. However, this is not true for the systems with the admixtures, as shown in Fig.5. Taking account of the FKG inequality saying that the entire conductance would be jointly contributed from fine and coarse paths [11], connectivity at a scale of fine porosity is lower in fly ash and silica fume systems even when the coarse porosity and its continuity are greater than the plain. Then, pore connectivity in the systems with the admixtures is still an increasing function of fine porosity, as found in Figs.6 and 7. However, a fine pore network is more disconnected in the systems with the admixtures. In other word, fine pores in the admixture-containing systems are more random such that they have less spatial correlation. This does not contradict shifting of the MIP curve toward a smaller diameter when those admixtures are incorporated. Reduction in conductivity by the mineral admixtures resulted from evolution of more discontinuous and random networks of fine capillary pores.

CONCLUSIONS

(1) Coarse capillary porosity is positively correlated to the electrical conductivity. Coarse pores work as effective backbone paths in conductivity.

(2) Fine capillary pore structure seems to have a similarity in geometrical features to the coarse structure in ordinary cement pastes. Connectivity between fine pores is an increasing function of the fine porosity. The fine pore structure does not contradict coarse pore structure that is decisive of transport properties.

(3) When mineral admixtures are used, coarse capillary pore structure is less dominant in determining conductivity. They decreased probability of connectedness of fine pores to the effective backbone path of conductivity.

ACKNOWLEDGEMENT

This work was supported by JSPS KAKENHI Grant Numbers 21560482 and 24560564.

REFERENCES

1. Wong, H.S., Buenfeld, N.R. and Head, M.K., Estimating transport properties of mortars using image analysis on backscattered electron images, Cement and Concrete Research, Vol.36, No.8, 2006, pp.1556-1566.
2. Katz, A.J. and Thompson, A.H., Prediction of rock electrical conductivity from mercury injection measurements, Journal of Geophysical Research, Vol.92, No.B1, 1987, pp.599-607.
3. Nokken, M.R. and Hooton, R.D., Electrical conductivity testing, Concrete International, Vol.28, No.10, 2006, pp.58-62.
4. Taylor, H.F.W., A method for predicting alkali ion concentrations in cement pore solutions, Advances in Cement Research, Vol.1, No.1, 1987, pp.1-6.
5. Snyder, K.A. et al., Estimating the electrical conductivity of cement paste pore solutions from OH^-, K^+ and Na^+ concentrations, Cement and Concrete Research, Vol.33, No.6, 2003, pp.793-798.
6. Kobayakawa, M. et al., Pozzolanic reaction of fly ash cement system, Proc. of 11st international congress on the chemistry of cement, Vol.2, 2003, pp.736-746.
7. Young, J.F. and Hansen, W., Volume relationships for CSH formation based on hydration stoichiometry, MRS Symposium Proc., Vol.85, 1987, pp.313-332.
8. Coker, D. A. and Torquato, S., Morphology and physical properties of Fontainebleau sandstone via a tomographic analysis, Journal of Geophysical Research, Vol.101, No.B8, 1996, pp.17497-17506.
9. Bentz, D.P. and Garboczi, E.J.: Percolation of phases in a three-dimensional cement paste microstructural model, Cement and Concrete Research, Vol.21, No.2/3, 1991, pp.325-344.
10. Garboczi, E. J.: Permeability, diffusivity, and microstructural parameters: A critical review, Cement and Concrete Research, Vol.20, No.4, 1990, pp.591-601.
11. Grimmett, G.: Percolation, second edition, Springer, Berlin Heidelberg, 1999.